Improved Thermal Interfaces of GaN–Diamond Composite Substrates for HEMT Applications

Jungwan Cho, Zijian Li, Elah Bozorg-Grayeli, Takashi Kodama, Daniel Francis, Felix Ejeckam, Firooz Faili, Mehdi Asheghi, and Kenneth E. Goodson

***Abstract*— High-power operation of AlGaN/GaN high-electron-mobility transistors (HEMTs) requires efficient heat removal through the substrate. GaN composite substrates, including the high-thermal-conductivity diamond, are promising, but high thermal resistances at the interfaces between the GaN and diamond can offset the benefit of a diamond substrate. We report on measurements of thermal resistances at GaN–diamond interfaces for two generations (first and second) of GaN-on-diamond substrates, using a combination of picosecond time-domain thermoreflectance (TDTR) and nanosecond transient thermoreflectance techniques. Two flipped-epitaxial samples are presented to determine the thermal resistances of the AlGaN/AlN transition layer. For the second generation samples, electrical heating and thermometry in nanopatterned metal bridges confirms the TDTR results. This paper demonstrates that the latter generation samples, which reduce the AlGaN/AlN transition layer thickness, result in a strongly reduced thermal resistance between the GaN and diamond. Further optimization of the GaN–diamond interfaces should provide an opportunity for improved cooling of HEMT devices.**

***Index Terms*— AlGaN/GaN high-electron-mobility transistors (HEMTs), thermal boundary resistance (TBR), thermal conductivity, time-domain thermoreflectance (TDTR).**

I. Introduction

HIGH-ELECTRON-MOBILITY transistors (HEMTs) based on AlGaN/GaN are promising for high-power high-frequency transistors and optoelectronic devices due to their high electron sheet charge densities and high electrical breakdown fields [1]. High-power operation exceeding 40 W/mm has been recently reported for a GaN-on-SiC configuration [2]. But localized device-level self-heating limits the peak power density and degrades device reliability [3]. The low thermal conductivity of the GaN buffer layer and the high thermal boundary resistances (TBRs) at interfaces in some composite substrates impede efficient heat dissipation from the heated device region.

Integration of diamond films and composite diamond substrates within micrometers of active regions can be a compelling materials solution since a polycrystalline diamond can have a thermal conductivity in the range 800–1800 W/mK [4], which is much higher than those of SiC (∼400 W/mK) and sapphire (∼35 W/mK). Recent efforts have used chemical-vapor-deposited (CVD) diamond substrates for AlGaN/GaN HEMTs [4]–[7]. The AlGaN/GaN epitaxial layers were first grown on a Si substrate by metal–organic chemical vapor deposition (MOCVD), and then atomically attached to a CVD polycrystalline diamond [4]. Another study reported AlGaN/GaN heterostructures grown on (111) single crystal diamond substrate by molecular beam epitaxy (MBE) [8].

Thermal properties in diamond-based composite substrates have received much less attention. These composite substrates require careful attention to thermal resistances between the GaN and diamond, which can diminish the benefits of using the high conductivity material. Kuzmik *et al.* [9] used an optical transient interferometric mapping (TIM) technique to estimate the thermal resistance very approximately at the GaN–diamond interface for MBE-grown GaN on single crystalline diamond. They reported an upper bound (< 10 m^{2}K/GW) for the interface resistance [9]. But they provided no explanation for this relatively low TBR at the GaN–diamond interface, and they did not assess the quality of their GaN buffer. Also, their previous work [10] on a GaN-on-SiC substrate showed that their TIM approach has a large degree of uncertainty for extracting TBR ($\pm$ 50%).

In this paper, we extract the thermal resistances between the GaN and diamond for two types of GaN-on-diamond substrates (first and second generation) at room temperature, using a combination of picosecond time-domain thermoreflectance (TDTR) and nanosecond transient thermoreflectance (TTR) techniques. Independent DC joule heating measurements with nanopatterned bridges confirm the TDTR results for the latter generation samples. We compare the thermal resistances at the GaN–diamond interfaces between the two generations, and show progress in reducing the GaN–diamond thermal interface resistance.

II. Samples and Experimental Methods

Fig. 1 illustrates the first and second generation GaN-on-diamond substrates used in this paper. For both generations

Manuscript received March 1, 2012; revised August 3, 2012; accepted August 30, 2012. Date of publication December 11, 2012; date of current version January 4, 2013. This work was supported by the DARPA Microsystems Technology Office through the U.S. Air Force under Contract FA8650-10-7044. The work of J. Cho was supported by the Samsung Scholarship. The work of Z. Li was supported by the Stanford Graduate Fellowship. The work of E. Bozorg-Grayeli was supported by the National Defense Science and Engineering Graduate Fellowship. Recommended for publication by Associate Editor R. Prasher upon evaluation of reviewers' comments.

J. Cho, Z. Li, E. Bozorg-Grayeli, T. Kodama, M. Asheghi, and K. E. Goodson are with the Department of Mechanical Engineering, Stanford University, Stanford, CA 94305 USA (e-mail: jungwan.cho@stanford.edu; lizj@stanford.edu; ebozorgg@stanford.edu; kodama@stanford.edu; mehdi@stanford.edu; goodson@stanford.edu).

D. Francis, F. Faili, and F. Ejeckam are with Group4 Labs, Inc., Fremont, CA 94539 USA (e-mail: daniel_francis@group4labs.com; firooz_faili@group4labs.com; felix_ejeckam@group4labs.com).

Color versions of one or more of the figures in this paper are available online at http://ieeexplore.ieee.org.

Digital Object Identifier 10.1109/TCPMT.2012.2223818

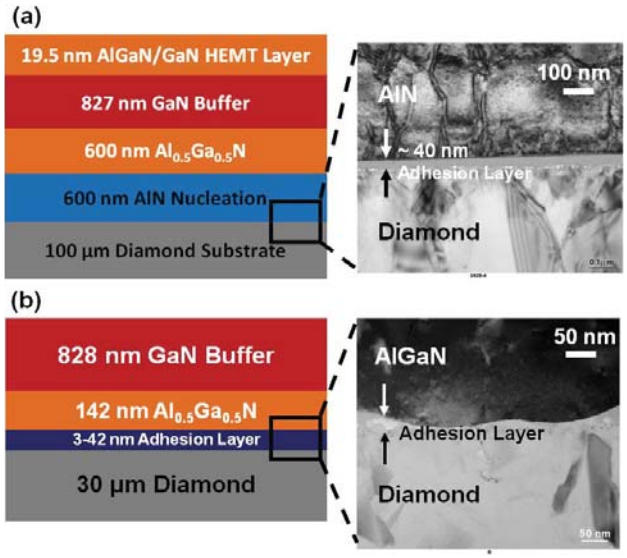

Fig. 1. Cross-sectional schematic drawings of the GaN-on-diamond substrates with representative cross-sectional TEMs near the adhesion layer. (a) First generation with a 1200-nm-thick $Al_{0.5}Ga_{0.5}N$/AlN transition layer. (b) Second generation with a significantly reduced transition layer (142-nm $Al_{0.5}Ga_{0.5}N$ for sample A and 269-nm $Al_{0.5}Ga_{0.5}N$ for sample B).

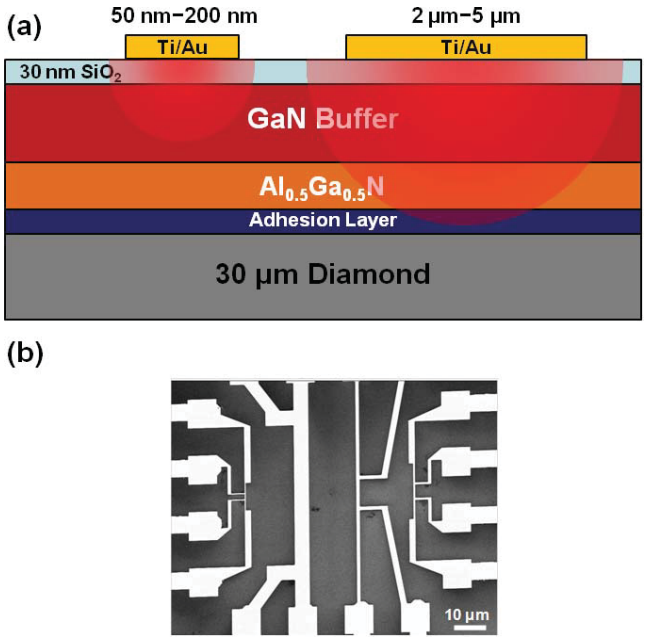

Fig. 2. (a) Electrical joule-heating and thermometry using patterned nanoheaters limits the heated region to the depth roughly scaled by the width of the bridge. This allows extraction of the thermal properties of the layers that are located within the volume of the heated region. (b) Top view of the nanoheaters fabricated using e-beam lithography (scanning electron microscopy image). Heater width varies from 50 nm to 5 μm. There are four V and I access pads for each bridge.

of samples, the AlGaN/GaN heterostructure was grown on a Si substrate by MOCVD. Following the MOCVD growth, this wafer was front-side mounted to a sacrificial carrier, and the Si substrate was etched away. The remaining AlGaN/GaN layers were attached to polycrystalline diamond using a disordered adhesion layer of thickness (~50 nm) as described previously [4]. The first generation GaN-on-diamond substrate has a 1200-nm-thick transition layer consisting of a 600-nm $Al_{0.5}Ga_{0.5}N$ and a 600-nm AlN layer to reduce the effects of lattice mismatch between the substrate and the GaN buffer layer. The second generation targets a substantial reduction in thermal resistance by reducing the AlGaN transition layer thickness by approximately 75% and completely removing the AlN nucleation layer. Cross-sectional transmission electron microscopy (TEM) images confirm the sample dimensions for both types of samples.

Picosecond TDTR and nanosecond TTR thermometries determine the thermal properties of these composite substrates. Both techniques extract normalized temperature decay for a heated metal transducer film on a stack of thin film materials, since metals exhibit linear changes in reflectivity with temperature for small temperature rises [11]. Picosecond TDTR [12]–[15] thermometry uses shorter timescales to determine near-surface thermal conductivities and interface resistances in multilayer thin film structures. A passively mode-locked Nd:YVO4 laser with an 82-MHz repetition rate generates 9.2-ps pulses at wavelength $\lambda = 1064$ nm. A beamsplitter separates these pulses into pump and probe components. The frequency-doubled pump beam, modulated by an electro-optic modulator (EOM) for lock-in detection, deposits heat in the metal transducer. The probe beam is temporally delayed from the pump by a linear delay stage, and the beam measures the surface temperature decay over 3.5 ns. A 3-D radial symmetric heat diffusion solution for the multilayer stack is fitted to the normalized temperature decay to extract the properties of films beneath the metal transducer [12]. We validate system accuracy by extracting a thermal conductivity of 1.38 W/mK for a SiO_2 calibration sample.

Nanosecond TTR thermometry [16], [17] uses longer timescales to investigate average transport properties within the material stack. Three-mm diameter, 532-nm wavelength, 6-ns pulses from a Nd:YAG laser heat the metal transducer at a repetition rate of 10 Hz, while a ~20-μm diameter, 658-nm continuous wave probe beam is focused on the metal surface in the middle of the pump beam. A 650-MHz photodiode and oscilloscope capture the transient temperature rise at the surface for several microseconds after the pulse. The analytical heat transfer model assumes 1-D heat conduction since the pump beam waist is significantly larger than the thermal diffusion depth during the measurement.

Electrical joule-heating and thermometry using patterned nanoheaters [18] helps to investigate and verify the thermal properties of the GaN-on-diamond substrates. We fabricated nanoheaters with four-probe configuration with widths varying from 50 nm to 5 μm on top of the sample stack (see Fig. 2). The heaters consist of 5-nm Ti and 50-nm Au, and are patterned using e-beam photolithography. The electrical thermometry captures the temperature rise by monitoring the electrical resistance change in the nanoheaters. Since the temperature coefficient of resistivity (TCR) of Au is dependent on film thickness partly due to the electron scattering at film boundaries, a calibration is performed before each measurement. Different heater widths spatially confine the heat to a certain depth into the sample stack [as shown in

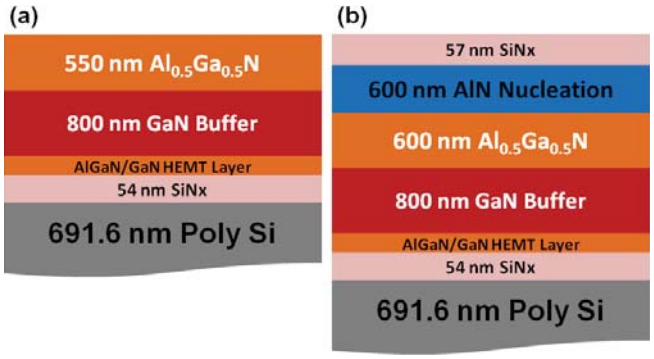

Fig. 3. Cross-sectional schematic drawings of the flipped-epitaxial samples. (a) AlGaN transition layer. (b) AlN nucleation layer.

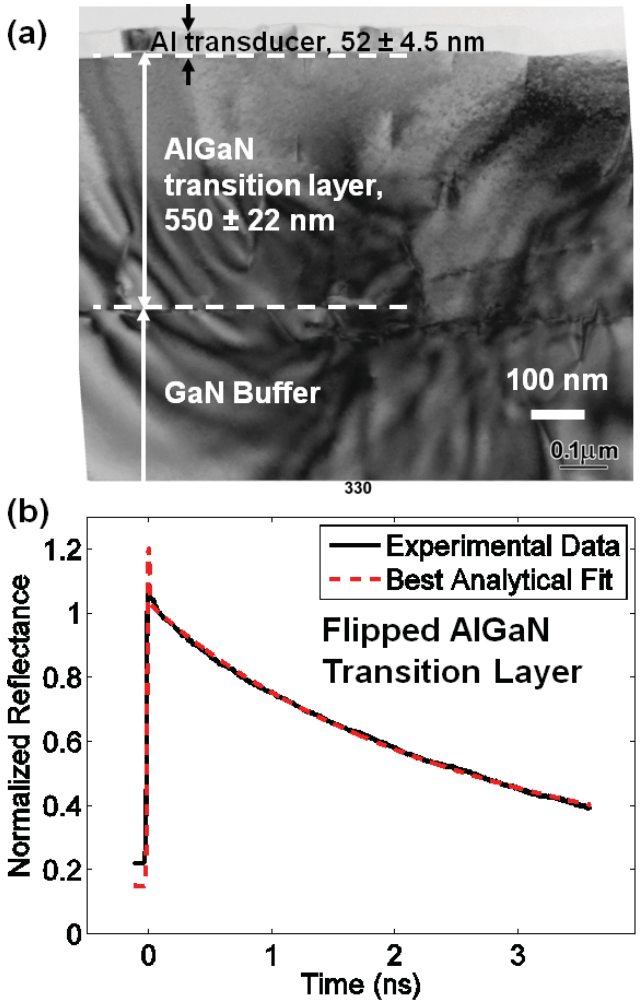

Fig. 4. (a) Representative cross-sectional TEM. (b) Thermal trace with data fit for flipped AlGaN transition layer.

Fig. 2(a)], which yields optimal sensitivity to different layers and interfaces. Specifically, the sub-micrometer narrow heater confines the heat within a very shallow region with DC joule heating, while the wide heaters (5 μm) generate near 1-D heat conduction through the films and are, therefore, sensitive to the bottom thermal resistances. Measurement data are fitted to a multilayer heat diffusion model to deduce the thermal properties of the underlying material.

For the first generation GaN-on-diamond substrate, picosecond TDTR measurement is not sensitive enough to probe the resistance of the transition layer and the adhesion layer, since these layers are placed deep within the material stack. Thus, specialized samples were prepared using a flipped-epitaxy technique. For this sample geometry, the entire structure is flipped, with the flipped AlGaN/GaN heterostructure resting on a structure consisting of SiN_x and polysilicon (see Fig. 3). Etching through the transition layer offers access to the $Al_{0.5}Ga_{0.5}N$ [see Fig. 3(a)] and the AlN [see Fig. 3(b)] by direct probing with picosecond TDTR. For the flipped AlN sample, the sample processing method left an additional 57 nm of SiN_x on the surface of the sample [see Fig. 3(b)].

III. Results and Discussion

A. First Generation GaN-on-Diamond Substrate

For the first generation GaN-on-diamond substrate, the thermal resistances between the GaN and diamond ($R_{\mathrm{GaN-diamond}}$) consist of three components: the $Al_{0.5}Ga_{0.5}N$ intrinsic resistance (R_{AlGaN}), the AlN intrinsic resistance (R_{AlN}), and the thermal resistance of the adhesion layer (R_{ADH}): $R_{\mathrm{GaN-diamond}} = R_{\mathrm{AlGaN}} + R_{\mathrm{AlN}} + R_{\mathrm{ADH}}$. The intrinsic resistances of the AlGaN and the AlN are determined by measuring two flipped-epitaxial samples with picosecond TDTR. Evaporated Al layers of 52 and 52.6 nm serve as the transducers for picosecond TDTR measurements on the flipped AlGaN and AlN samples, respectively. The Al layer thicknesses for these samples were confirmed using cross-sectional TEM images [see Figs. 4(a) and 5(a)]. We use nanosecond TTR to measure the thermal resistance of the adhesion layer of the first generation GaN-on-diamond substrate coated with 150-nm Cr/100 nm Ti.

Fig. 4 shows a representative TEM image and the thermal trace with the best analytical fit for the flipped $Al_{0.5}Ga_{0.5}N$ sample. Data are fit assuming a semi-infinite behavior of the $Al_{0.5}Ga_{0.5}N$ transition layer since the thermal diffusion depth of 457 nm in the layer at 5-MHz pump modulation frequency is smaller than the layer thickness. The AlGaN heat capacity is assumed to be similar to that of GaN, which is taken from the literature [19]. The measurement is sensitive to the TBR between the Al transducer and the $Al_{0.5}Ga_{0.5}N$ layer ($R_{\mathrm{Al-AlGaN}}$), and to the thermal conductivity of the $Al_{0.5}Ga_{0.5}N$ layer (k_{AlGaN}). At room temperature, we find $k_{\mathrm{AlGaN}} = 16.6 \pm 3.2$ W/mK and $R_{\mathrm{Al-AlGaN}} = 21 \pm 2.3$ m^{2}K/GW. The error bars are due to uncertainty in the Al transducer thickness ($d_{\mathrm{Al}} = 52.0 \pm 4.5$ nm).

Daly *et al.* [20] used TDTR thermometry to extract $Al_xGa_{1-x}N$ thermal conductivity values that varied with the Al mass fraction (x) and temperature. At room temperature, these authors [20] found that the thermal conductivity of the polycrystalline $Al_{0.44}Ga_{0.56}N$ film grown by MOCVD on a sapphire substrate was around 6 W/mK, which is smaller than the measured thermal conductivity of the $Al_{0.5}Ga_{0.5}N$ film in this paper. Liu *et al.* [21] did a similar study to measure the $Al_xGa_{1-x}N$ thermal conductivities using the 3ω method. They measured the thermal conductivity of the $Al_{0.4}Ga_{0.6}N$

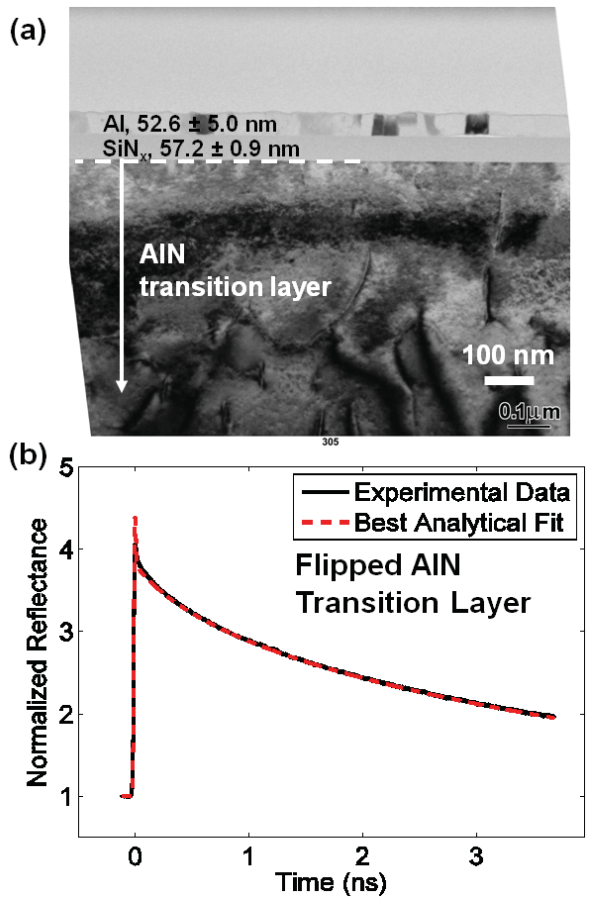

Fig. 5. (a) Representative cross-sectional TEM. (b) Thermal trace with data fit for flipped AlN transition layer.

film grown by hydride vapor-phase epitaxy on a c-plane sapphire substrate. Their measured room-temperature thermal conductivity was 25 W/mK, which is somewhat larger than the room temperature data in this paper. The difference may be due to the crystalline quality of the AlGaN alloy, which depends on growth processes and growth substrates.

Fig. 5 illustrates a representative cross-sectional TEM image and the thermal trace with the best analytical fit for the flipped AlN sample. The measurement is sensitive to the TBR between the Al transducer and the SiN layer ($R_{\mathrm{Al-SiN}}$), to the thermal conductivity of the SiN layer (k_{SiN}), and to the thermal conductivity of the AlN layer (k_{AlN}). Since the TBRs between the layers ($R_{\mathrm{SiN-AlN}}$ and $R_{\mathrm{AlN-AlGaN}}$) are convolved into k_{SiN} and k_{AlN}, we can extract only the effective thermal conductivity of each layer. The SiN and AlN heat capacities are taken from the literature [22], [23]. At room temperature, we find $R_{\mathrm{Al-SiN}} = 10.9 \pm 0.6$ m^{2}K/GW, $k_{\mathrm{SiN}} = 2.2 \pm 0.4$ W/mK, and $k_{\mathrm{AlN}} = 30.5 \pm 5.0$ W/mK. The error bars are due to variation in the thickness of the Al transducer ($d_{\mathrm{Al}} = 52.6 \pm 5.0$ nm). Manoi *et al.* [24] used micro Raman thermometry to investigate thermal conductivity values of MOCVD-grown AlN nucleation layers for GaN-on-SiC substrates. They found that the AlN thermal conductivities range between 1.5 and 23 W/mK at room temperature depending on crystalline quality and thickness of the AlN nucleation layer. A general trend of increasing AlN thermal conductivity with thickness was observed in their work, from an average of 2.2 W/mK for 40-nm-thick layers to 14.3 W/mK for 200-nm-thick layers. Their maximum AlN thermal conductivity of 23 W/mK for a 200-nm-thick layer is comparable to our value of 30.5 W/mK, considering that the AlN has better crystalline quality with increasing layer thickness.

TABLE I
GEOMETRIES AND THICKNESSES FOR SECOND GENERATION GaN-ON-DIAMOND SUBSTRATES

Samples	GaN Thickness [nm]	$Al_{0.5}Ga_{0.5}N$ Thickness [nm]	Adhesion Layer Thickness [nm]
A	828	142	3–42
B	848	269	38–55

The dominant source of experimental uncertainty in the picosecond TDTR measurement is due to variation in the thickness of the Al transducer. For the material stacks in this paper, the uncertainties due to multiple spot measurements lie within the error bars due to variation in the Al thickness. Also, small variations in heat capacity values have little influence on the fitted parameters.

Nanosecond TTR measurement determines the room temperature thermal resistance of the adhesion layer (R_{ADH}) in the first generation GaN-on-diamond substrate. The measurement is sensitive to the effective thermal conductivity (k_{eff}) of the lumped stack, which includes a 20-nm HEMT layer, an 800-nm GaN buffer, and a 1200-nm transition layer, and to the thermal resistance of the adhesion layer (R_{ADH}). The best analytical fit to the measured data yields an effective thermal conductivity of $\sim 18.1 \pm 6.5$ W/mK. R_{ADH} is estimated to be 52 ± 15 m^{2}K/GW. The large uncertainties in R_{ADH} ($\sim$30%) are due to the following factors: 1) the complexity of the structure and oversimplification in thermal modeling; 2) spatial variations in thermal conductivity across various layers; and 3) the presence of multiple interfaces.

B. Second Generation GaN-on-Diamond Substrate

We perform picosecond TDTR measurements on the two second generation GaN-on-diamond substrates (samples A and B) to extract the thermal resistances between the GaN and diamond. Table I summarizes sample dimensions, which were confirmed by cross-sectional TEM images. The thermal resistances between the GaN and diamond ($R_{\mathrm{GaN-diamond}}$) consist of two components: the $Al_{0.5}Ga_{0.5}N$ intrinsic resistance (R_{AlGaN}) and the thermal resistance of the adhesion layer (R_{ADH}): $R_{\mathrm{GaN-diamond}} = R_{\mathrm{AlGaN}} + R_{\mathrm{ADH}}$. Here, the intrinsic resistance of the adhesion layer and the TBRs at its boundaries are lumped into a single resistance (R_{ADH}).

The measurements aim at extracting the thermal resistances of the adhesion layers (R_{ADH}) in both samples. To accurately determine these values, all other thermal parameters must be known. We use the electrical thermometry to independently measure the thermal conductivity of the GaN buffer layer. The narrow heaters (50–200 nm) confine the heat within the top layers, and, hence, the temperature rise in the heater is

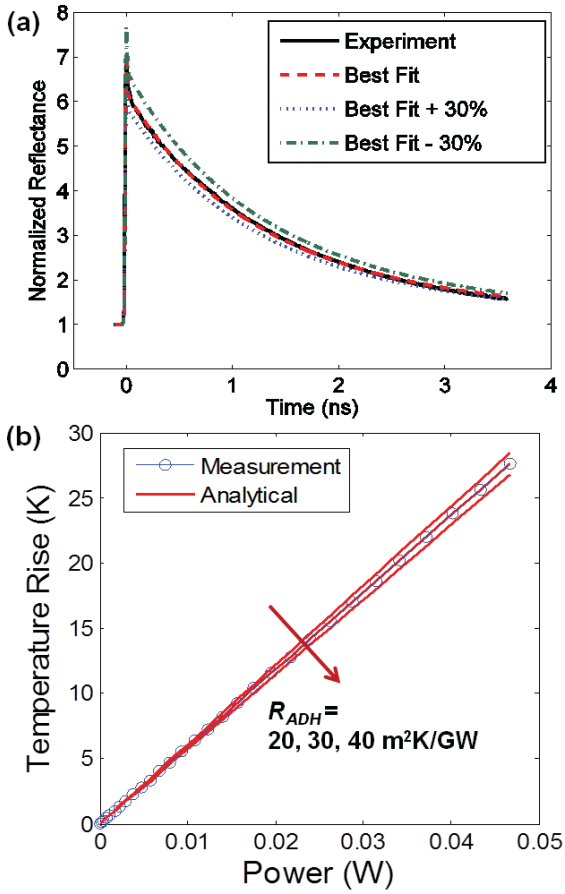

Fig. 6. (a) Normalized TDTR thermal trace along with best-fit analytical curve ($R_{\mathrm{ADH}} = 27$ m^{2}K/GW) for sample A. The blue dotted and green dashed-dotted curves illustrate the data extraction sensitivity, showing the analytical fits obtained by varying the best-fit value (R_{ADH}) by $\pm$ 30%. (b) Data fitting process for R_{ADH} in electrical joule-heating and thermometry. For both techniques, all material properties except R_{ADH} are obtained independently through TDTR or separate joule heating measurements.

most sensitive to the thermal conductivity of the GaN. This measurement yields $k_{\mathrm{GaN}} = 80 \pm 10$ W/mK. For the thermal conductivity of the $Al_{0.5}Ga_{0.5}N$ film, we utilize our measurement of the flipped AlGaN sample (see Section III.A). The diffuse mismatch model [25], [26] predicts the GaN/AlGaN TBR to be 0.8 m^{2}K/GW. Small variations in the GaN/AlGaN TBR have little influence on the data extraction. Since diamond has very high thermal conductivity (both out-of-plane and in-plane) and is buried below the stack, the current picosecond TDTR and nanosecond TTR measurements are not sensitive to the diamond thermal conductivity and its conductivity anisotropy. The diamond thermal conductivity, conductivity anisotropy, and heat capacity are taken from the literature [27], [28].

Table II summarizes all the measured values in both samples. Picosecond TDTR measurements determine that the thermal resistances of the adhesion layer range from 17 to 42 m^{2}K/GW. Further, we find the TBRs between the Al transducer and GaN buffer layer ($R_{\mathrm{Al-GaN}}$) to be 10.6 $\pm$ 1.2 m^{2}K/GW for sample A and 10.2 $\pm$ 1.2 m^{2}K/GW for sample B. The uncertainty bars in these results are due to the effects of the Al transducer thickness ($d_{\mathrm{Al}} = 51.0 \pm 3.5$ nm).

TABLE II
THERMAL RESISTANCES OF ADHESION LAYERS FOR SECOND GENERATION GaN-ON-DIAMOND SUBSTRATES

Measurement Technique	$R_{\mathrm{ADH,A}}$ [m^{2}K/GW]	$R_{\mathrm{ADH,B}}$ [m^{2}K/GW]
Picosecond TDTR	27 $\pm$ 10	31 $\pm$ 11
DC joule heating	25 $\pm$ 11	29 $\pm$ 12

TABLE III
GaN–DIAMOND THERMAL INTERFACE RESISTANCES FOR FIRST AND SECOND GENERATION GaN-ON-DIAMOND SUBSTRATES

	R_{AlGaN} [m^{2}K/GW]	R_{AlN} [m^{2}K/GW]	R_{ADH} [m^{2}K/GW]	$R_{\mathrm{GaN-diamond}}$ [m^{2}K/GW]
First gen	36 $\pm$ 8	20 $\pm$ 4	52 $\pm$ 15	108 $\pm$ 27
Second gen, Sample A	9 $\pm$ 2	N/A	27 $\pm$ 10	36 $\pm$ 12
Second gen, Sample B	16 $\pm$ 4	N/A	31 $\pm$ 11	47 $\pm$ 15

We perform DC joule heating measurements on the same samples to verify the TDTR results. Wider heaters (2 μm–5 μm) generate heat that penetrates deep into the layer stack and therefore capture the adhesive thermal resistance [see Fig. 6(b)]. The measured thermal resistances at room temperature agree with the TDTR results within uncertainties (see Table II).

IV. CONCLUSION

The thermal resistances between the GaN and diamond ($R_{\mathrm{GaN-Diamond}}$) were measured for both first and second generation GaN-on-diamond substrates, using a combination of picosecond TDTR and nanosecond TTR techniques. Table III summarizes all the measurements for both first and second generation samples. For the first generation samples, picosecond TDTR measurements on the two flipped-epitaxial samples determined the thermal resistances of the AlGaN and AlN films (R_{AlGaN} and R_{AlN}). Nanosecond TTR measurement extracted the thermal resistance of the adhesion layer (R_{ADH}). For the second generation samples, the thermal resistances of the adhesion layers (R_{ADH}) in two samples were extracted using picosecond TDTR. Independent DC joule heating measurements on the same samples confirmed the TDTR results. Utilizing k_{AlGaN} taken from the measurement on the flipped AlGaN sample, we determined the intrinsic resistance of the AlGaN layer.

As Table III shows, the second generation GaN-on-diamond substrates significantly reduced GaN-diamond thermal interface resistances, which are less than half of that of the first generation sample. We can achieve a more reduced GaN–diamond thermal interface resistance by further etching the residual AlGaN layer. Our efforts for reducing the transition layer thickness target a reduction of the thermal resistance. This reduction of the GaN–diamond thermal interface resistance is required to obtain the expected benefits of using

the high thermal conductivity diamond. Recent simulation work has shown that the complete removal of the 1-μm transition layer reduces the temperature rise of the GaN-on-diamond configuration by up to 50% [29]. In this simulation, Li *et al.* [29] demonstrated that HEMT-on-diamond with a GaN–diamond thermal interface resistance of < 30 m^{2}K/GW can outperform HEMT-on-SiC even with zero GaN–SiC thermal interface resistance in terms of device temperature rise [29]. Therefore, a further reduction in the GaN–diamond thermal interface resistance should be achieved and should eventually enhance cooling of HEMT-on-diamond devices.

REFERENCES

[1] U. K. Mishra, P. Parikh, and Y. F. Wu, "AlGaN/GaN HEMTs-an overview of device operation and applications," *Proc. IEEE*, vol. 90, no. 6, pp. 1022–1031, Jun. 2002.

[2] Y. F. Wu, M. Moore, A. Saxler, T. Wisleder, and P. Parikh, "40-W/mm double field-plated GaN HEMTs," in *Proc. 64th Device Res. Conf.*, Jun. 2006, pp. 151–152.

[3] G. Meneghesso, G. Verzellesi, F. Danesin, F. Rampazzo, F. Zanon, A. Tazzoli, M. Meneghini, and E. Zanoni, "Reliability of GaN high-electron-mobility transistors: State of the art and perspectives," *IEEE Trans. Device Mater. Rel.*, vol. 8, no. 2, pp. 332–343, Jun. 2008.

[4] D. Francis, F. Faili, D. Babic, F. Ejeckam, A. Nurmikko, and H. Maris, "Formation and characterization of 4-inch GaN-on-diamond substrates," *Diam. Rel. Mater.*, vol. 19, pp. 229–233, Feb. 2010.

[5] J. G. Felbinger, M. V. S. Chandra, Y. Sun, L. F. Lester, J. Wasserbauer, F. Faili, D. Babic, D. Francis, and F. Ejeckman, "Comparison of GaN HEMTs on diamond and SiC substrates," *IEEE Electron Device Lett.*, vol. 28, no. 11, pp. 948–950, Nov. 2007.

[6] K. D. Chabak, J. K. Gillespie, V. Miller, A. Crespo, J. Roussos, M. Trejo, D. E. Walker, Jr., G. D. Via, G. H. Jessen, J. Wasserbauer, F. Faili, D. I. Babic, D. Francis, and F. Ejeckam, "Full-wafer characterization of AlGaN/GaN HEMTs on free-standing CVD diamond substrates," *IEEE Electron Device Lett.*, vol. 31, no. 2, pp. 99–101, Feb. 2010.

[7] Q. Diduck, J. Felbinger, L. F. Eastman, D. Francis, J. Wasserbauer, F. Faili, D. I. Babic, and F. Ejeckam, "Frequency performance enhancement of AlGaN/GaN HEMTs on diamond," *Electron. Lett.*, vol. 45, no. 14, pp. 758–759, Jul. 2009.

[8] M. Alomari, A. Dussaigne, D. Martin, N. Grandjean, C. Gaquiere, and E. Kohn, "AlGaN/GaN HEMT on (111) single crystalline diamond," *Electron. Lett.*, vol. 46, no. 4, pp. 299–301, Feb. 2010.

[9] J. Kuzmik, S. Bychikhin, D. Pogany, E. Pichonat, O. Lancry, C. Gaquiere, G. Tsiakatouras, G. Deligeorgis, and A. Georgakilas, "Thermal characterization of MBE-grown GaN/AlGaN/GaN device on single crystalline diamond," *J. Appl. Phys.*, vol. 109, pp. 086106-1–086106-3, Apr. 2011.

[10] J. Kuzmik, S. Bychikhin, D. Pogany, C. Gaquiere, E. Pichonat, and E. Morvan, "Investigation of the thermal boundary resistance at the III-nitride/substrate interface using optical methods," *J. Appl. Phys.*, vol. 101, no. 5, pp. 054508-1–054508-6, Mar. 2007.

[11] K. Ujihara, "Reflectivity of metals at high temperature," *J. Appl. Phys.*, vol. 43, no. 5, pp. 2376–2383, May 1972.

[12] D. G. Cahill, "Analysis of heat flow in layered structures for time-domain thermoreflectance," *Rev. Sci. Instrum.*, vol. 75, no. 12, pp. 5119–5122, Nov. 2004.

[13] M. A. Panzer, M. Shandalov, J. A. Rowlette, Y. Oshima, Y. W. Chen, P. C. McIntyre, and K. E. Goodson, "Thermal properties of ultrathin hafnium oxide gate dielectric films," *IEEE Electron Device Lett.*, vol. 30, no. 12, pp. 1269–1271, Dec. 2009.

[14] J. P. Reifenberg, K. W. Chang, M. Panzer, S. B. Kim, J. A. Rowlette, M. Asheghi, H. S. P. Wong, and K. E. Goodson, "Thermal boundary resistance measurements for phase-change memory devices," *IEEE Electron Device Lett.*, vol. 31, no. 1, pp. 56–58, Jan. 2010.

[15] J. Cho, E. Bozorg-Grayeli, D. H. Altman, M. Asheghi, and K. E. Goodson, "Low thermal resistances at GaN–SiC interfaces for HEMT technology," *IEEE Electron Device Lett.*, vol. 33, no. 3, pp. 378–380, Mar. 2012.

[16] M. A. Panzer, G. Zhang, D. Mann, X. Hu, E. Pop, H. Dai, and K. E. Goodson, "Thermal properties of metal-coated vertically aligned single-wall nanotube arrays," *J. Heat Transfer*, vol. 130, pp. 052401-1–052401-9, May 2008.

[17] M. A. Panzer, H. M. Duong, J. Okawa, J. Shiomi, B. L. Wardle, S. Maruyama, and K. E. Goodson, "Temperature-dependent phonon conduction and nanotube engagement in metalized single wall carbon nanotube films," *Nano Lett.*, vol. 10, no. 7, pp. 2395–2400, May 2010.

[18] J. Lee, Z. Li, J. P. Reifenberg, S. Lee, R. Sinclair, M. Asheghi, and K. E. Goodson, "Thermal conductivity anisotropy and grain structure in $Ge_2Sb_2Te_5$ films," *J. Appl. Phys.*, vol. 109, no. 8, pp. 084902-1–084902-6, Apr. 2011.

[19] I. Zieborak-Tomaszkiewicz, E. Utzig, and P. Gierycz, "Heat capacity of crystalline GaN," *J. Thermal Anal. Calorimetry*, vol. 91, no. 1, pp. 329–332, 2008.

[20] B. C. Daly, H. J. Maris, A. V. Nurmikko, M. Kuball, and J. Han, "Optical pump-and-probe measurement of the thermal conductivity of nitride thin films," *J. Appl. Phys.*, vol. 92, no. 7, pp. 3820–3824, Oct. 2002.

[21] W. L. Liu and A. A. Balandin, "Thermal conduction in $Al_xGa_{1-x}N$ alloys and thin films," *J. Appl. Phys.*, vol. 97, no. 7, pp. 073710–073715, Apr. 2005.

[22] S. Bai, Z. Tang, Z. Huang, and J. Yu, "Thermal characterization of Si_3N_4 thin films using transient thermoreflectance technique," *IEEE Trans. Ind. Electron.*, vol. 56, no. 8, pp. 3238–3243, Aug. 2009.

[23] A. Al Shaikhi and G. P. Srivastava, "Specific heat calculations of III-N bulk materials," *Phys. Status Solidi C*, vol. 3, no. 6, pp. 1495–1498, Jun. 2006.

[24] A. Manoi, J. W. Pomeroy, N. Killat, and M. Kuball, "Benchmarking of thermal boundary resistance in AlGaN/GaN HEMTs on SiC substrates: Implications of the nucleation layer microstructure," *IEEE Electron Device Lett.*, vol. 31, no. 12, pp. 1395–1397, Dec. 2010.

[25] E. T. Swartz and R. O. Pohl, "Thermal boundary resistance," *Rev. Mod. Phys.*, vol. 61, no. 3, pp. 605–668, Jul. 1989.

[26] L. De Bellis, P. E. Phelan, and R. S. Prasher, "Variations of acoustic and diffuse mismatch models in predicting thermal-boundary resistance," *J. Thermophys. Heat Transfer*, vol. 14, no. 2, pp. 144–150, Apr.–Jun. 2000.

[27] J. E. Graebner, S. Jin, G. W. Kammlott, J. A. Herb, and C. F. Gardinier, "Large anisotropic thermal-conductivity in synthetic diamond films," *Nature*, vol. 359, pp. 401–403, Oct. 1992.

[28] J. E. Graebner, "Measurements of specific heat and mass density in CVD diamond," *Diam. Rel. Mater.*, vol. 5, no. 11, pp. 1366–1370, Nov. 1996.

[29] Z. Li, M. Asheghi, and K. E. Goodson, "Impact of composite substrates on near junction self heating of high electron mobility transistors," unpublished.

Jungwan Cho received the B.S. degree from Seoul National University, Seoul, Korea, in 2008, and the M.S. degree from Stanford University, Stanford, CA, in 2010, where he is currently pursuing the Ph.D. degree, all in mechanical engineering.

He is currently involved in characterizing thermal properties of AlGaN/GaN high electron mobility transistors, using nanosecond and picosecond thermoreflectance techniques. His current research interests include nanoscale transport phenomena in thin films and interfaces between various materials.

Mr. Cho was a recipient of the Kwanjeong Educational Foundation Fellowship and the Samsung Scholarship to support his M.S. and Ph.D. studies, respectively.

Zijian Li received the B.S. degree in precision instruments with a focus on microelectromechanical systems from Tsinghua University, Haidian, China, in 2008, and the M.S. degree in electrical engineering from Stanford University, Stanford, CA, in 2010, where he is currently pursuing the Ph.D. degree in mechanical engineering.

His current research interests include nanoscale thermal and electronic transport in phase change memory, high electron mobility transistors, and extreme ultraviolet mirror technology.

Mr. Li was a recipient of the Stanford Graduate Fellowship.

Elah Bozorg-Grayeli received the B.S. (Hons.) degree in mechanical engineering from the California Institute of Technology, Pasadena, in 2008, and the M.S. degree in mechanical engineering from Stanford University, Stanford, CA, in 2010, where he is currently pursuing the Ph.D. degree in mechanical and electrical engineering.

He is engaged in measuring thermal properties of materials used in phase change memory, high electron mobility transistors, and extreme UV mirrors, using nanosecond and picosecond thermoreflectance. His current research interests include understanding nanoscale heat conduction in thin films and in junctions between dissimilar materials.

Mr. Bozorg-Grayeli was a recipient of the National Defense Science and Engineering Graduate Fellowship and the Honorary Fellowship from Stanford University and the National Science Foundation.

Takashi Kodama received the B.S., M.S., and Ph.D. degrees in biomolecular engineering from the Tokyo Institute of Technology, Tokyo, Japan, in 2001, 2003, and 2006, respectively.

He is currently a Research Associate under the supervision of Prof. K. E. Goodson and is involved in research on electrothermal transport in nanomaterials. His current research interests include developing new scanning probe microscopes for several scientific applications.

Daniel Francis received the Ph.D. degree in applied physics, with a focus on semiconductor lasers, from Stanford University, Stanford, CA, in 1997.

He is currently the CTO of Group4 Labs, Inc., Fremont, CA, a material development company focused on the development of high-power electronic materials. He was a member of the Founding Team, Genoa Corp., a telecom start-up focused on materials and device innovations for the telecommunications industry. He was a Visiting Post-Doctoral Researcher with the University of California, Berkeley, in 1998, where he was engaged in research on semiconductor lasers. He has authored or co-authored more than 50 papers in refereed journals and conferences and holds 20 issued or pending patents.

Felix Ejeckam received the Ph.D. degree in electrical and computer engineering, with a focus on materials science and optoelectronics, from Cornell University, Ithaca, NY, in 1997.

He is a Co-Founder and the CEO of Group4 Labs, Inc., Fremont, CA, a company that develops GaN-on-diamond wafer technologies for RF, power, and photonics applications. He was a Co-Founder and the CEO of Nova Crystals, Inc., a company that developed next-generation DFB and APDs for telecom and datacom fiberoptics networks. He was an Associate with McKinsey & Company, Inc. New York, NY. He has authored or co-authored more than 50 papers in refereed journals and conferences, and holds more than 10 issued or pending patents.

Firooz Faili received the B.S. degree in chemical engineering from the Abadan Institute of Technology, Abadan, Iran, in 1977, the M.S. degree in chemical engineering from San Jose State University, San Jose, CA, in 1980, and the Ph.D. degree in chemical engineering from University of Southern California, Los Angeles, CA, in 1944.

He is currently the Vice President of Group4 Labs, Inc., Fremont, CA, a material development company focused on the development of high-power electronic materials. He has 20 years of experience on technology development for various small and large companies in the semiconductor industry. He was a Process Technologist with Varian Associates and involved in research on dielectric and conductor etching and CVD development, and was the Chief Technologist with LASA industries, where he was engaged in the development of new methodology for prototyping of ASICs. He has a wide range expertise in the fields of materials science and integration of multilevel interconnect, silicon and wide band-gap electronics, and thin- and thick-film processing.

Mehdi Asheghi received the Ph.D. degree from Stanford University, Stanford, CA, in 1999.

He is currently a Consulting Associate Professor with Stanford University, where he is engaged in further development of PCRAM technology. He led a well-known and funded research program from 2000 to 2006 at Carnegie Mellon University, Pittsburgh, PA, which focused on nanoscale thermal phenomena in semiconductor and data storage devices. He was a Post-Doctoral Researcher with Stanford University, where he was involved in research on nanoscale thermal engineering of microelectronic devices. He has authored or co-authored more than 110 reviewed papers in journals and conferences, and book chapters.

Dr. Asheghi was the Program Chair of ITHERM 2012 and the General Chair of ITHERM 2014.

Kenneth E. Goodson received the Ph.D. degree from the Massachusetts Institute of Technology (MIT), Cambridge, in 1993.

He is currently a Professor and the Vice Chair of Mechanical Engineering with Stanford University, Stanford, CA, where his group studies thermal phenomena in electronic nanostructures and energy conversion devices. He is a Founder and the former CTO of Cooligy, Inc., which builds microcoolers for computers and was acquired in 2005 by Emerson. He was a JSPS Visiting Professor with The Tokyo Institute of Technology. His Doctoral Alumni include Professors with the University of California, Berkeley, MIT, the University of California, Los Angeles, the University of Illinois at Urbana-Champaign, Urbana and the University of Michigan, Ann Arbor, as well as Staff Members with Intel, AMD, and IBM. He has authored or co-authored more than 120 archival journal articles, two books, and eight book chapters, and holds 24 patents.

Dr. Goodson was the recipient of the Allan Kraus Thermal Management Medal from the American Society of Mechanical Engineers (ASME), the Office of Naval Research Young Investigator Award, the National Science Foundation Career Award, the Outstanding Reviewer Award from the *ASME Journal of Heat Transfer*, for which he was an Associate Editor, and the Best Paper Award at SEMI-THERM, SRC TECHCON, and the IEDM. He is the Editor-in-Chief of *Nanoscale and Microscale Thermophysical Engineering*. His research has been recognized through keynote lectures at INTERPACK, ITHERM, and Therminic.